

# Tetragonal Structure Induced by Wetting at the Interface between a Solid Substrate and a Lyotropic Sponge Phase

M. Magalhães,<sup>†</sup> A. M. Figueiredo Neto,<sup>\*,†</sup> G. Barbero,<sup>‡</sup> and A. C. Tromba<sup>†</sup>

*Instituto de Física, Universidade de São Paulo, caixa postal 66318, 05315-970, São Paulo SP, Brazil, and Dipartimento di Fisica, Politecnico di Torino, and Istituto Nazionale di Fisica della Materia, Corso Duca degli Abruzzi 24, 10129 Torino, Italy*

*Received: May 14, 2003; In Final Form: October 3, 2003*

The wetting of a solid substrate by a lyotropic sponge phase is studied by using grazing X-ray scattering and optical microscopy. The wetting promotes the formation of an anisotropic layer of tetragonal symmetry on length scales of  $\sim 10$  nm on the substrate. The topology of the substrate defines the orientation of the symmetry axis of this induced surface layer. The shape anisotropy characteristics of the tetragonal lattice experimentally obtained account for the optical phase shift measured.

## Introduction

One of the most interesting optically isotropic phases encountered in some particular regions of the phase diagrams of lyotropic mixtures is the sponge phase (also named the  $L_3$  phase). Sponge phases have been observed in both water-rich and oil-rich mixtures, mostly in the vicinity of swollen lamellar phase domains.<sup>1</sup> Its structure is not long-range-ordered, and the experimental observations point toward a microstructure where a surfactant bilayer (thickness  $\delta$ ) of multiply connected topology (bicontinuous structure) separates two solvent domains over macroscopic distances.<sup>2</sup> To some extent, the structure of the  $L_3$  phase can be sketched as a melted cubic structure (with no long-range ordering) of "lattice parameter"  $d$ .<sup>3,4</sup> This picture was proposed for the sponge phase in the volume (i.e., without any external constraint). A remarkable characteristics of the  $L_3$  phase is the flow-induced (under shear or even a gentle shaking) birefringence.

In previous work,<sup>5</sup> we reported on a static effect that consists of inducing an anisotropic structure at the interface between a glass surface and a sponge phase. Our proposed interpretation assumed a surface-field-induced phase transition from the sponge phase to an anisotropic phase at the interface. At that time, however, no experimental evidence was available to determine the structure of this anisotropic induced phase at the interface. In the case of thermotropic liquid crystals, the wetting of solid substrates was shown to induce 2D and even 3D networks in a layer near the interface.<sup>6–8</sup>

In this work we present grazing X-ray scattering and complementary optical results that allow the determination of the structure of this wetting-induced anisotropic phase layer, show that its characteristic parameters account for the measured optical phase shift, and discuss the results in terms of elastic theory.

## Experimental Section

**Sample.** The lyotropic system investigated is a mixture of sodium dodecyl sulfate (SDS)/1-pentanol (POH)/cyclohexane

$C_6H_{12}$  ( $C_6$ )/water (W). The phase diagram of this quaternary system was partially explored,<sup>9</sup> and a sponge phase was identified in the  $C_6$ -rich, W-poor corner of an isothermal of the phase diagram. Let us call  $\phi_a$  the volume fraction of the amphiphile in the lyotropic mixture and  $[X]$  represents the percent molar concentration (M%) of substance X. We explored a linear path of the partial isothermal ( $T = 23 \pm 1$  °C) phase diagram at  $[SDS + POH] = 7.5$  and  $20 < [C_6] < 70$ . In the bulk, the results accumulated from the different experimental techniques point toward an inverted structure for the  $L_3$  phase over the entire the concentration range investigated for this partial isothermal.<sup>10</sup> In this structure, a water layer of thickness  $\delta$  ( $\sim 5$  nm) separates two unconnected regions with  $C_6$ . This water layer is separated from  $C_6$  by the polar heads of the SDS and OH groups of the POH molecules. The mean distance between the  $C_6$  channels is  $d \approx 20$  nm.

**X-ray Grazing Scattering Setup.** The grazing scattering experiments were performed in the synchrotron facility of the LNLS (Laboratório Nacional de Luz Sincrotron, Brazil) using X-ray wavelength  $\lambda = 0.148$  nm. In these experiments, the substrate of the sample holder cell in contact with the sponge phase is a beryllium plate 240  $\mu\text{m}$  thick, which also presents parallel channels (Figure 1A) with a larger (and less homogeneous) wavelength than that of the Teflon layer (Figure 1B). The X-ray beam is oriented at an angle of  $88.5^\circ$  with respect to the normal to the Be plate.

**Optical Setup.** The optical setup employed to measure the surface-field-induced phase shift is the same as that described in ref 5. It allows the simultaneous determination of the optical phase shift ( $\psi$ ) of the surface-induced anisotropic layer and the orientation of its optical axis with respect to the laboratory frame axes ( $\gamma_0$ ). The sample holder is made of two glass plates separated by a Teflon spacer that is 4 mm thick. One of the plates is recovered with a thin ( $\sim 0.1$   $\mu\text{m}$  thick) and transparent Teflon film deposited (stretched while hot) on it. This process forms periodic parallel channels on the Teflon surface, with a typical wavelength of  $\sim 0.2$   $\mu\text{m}$  (Figure 1B) along the  $x$  axis.

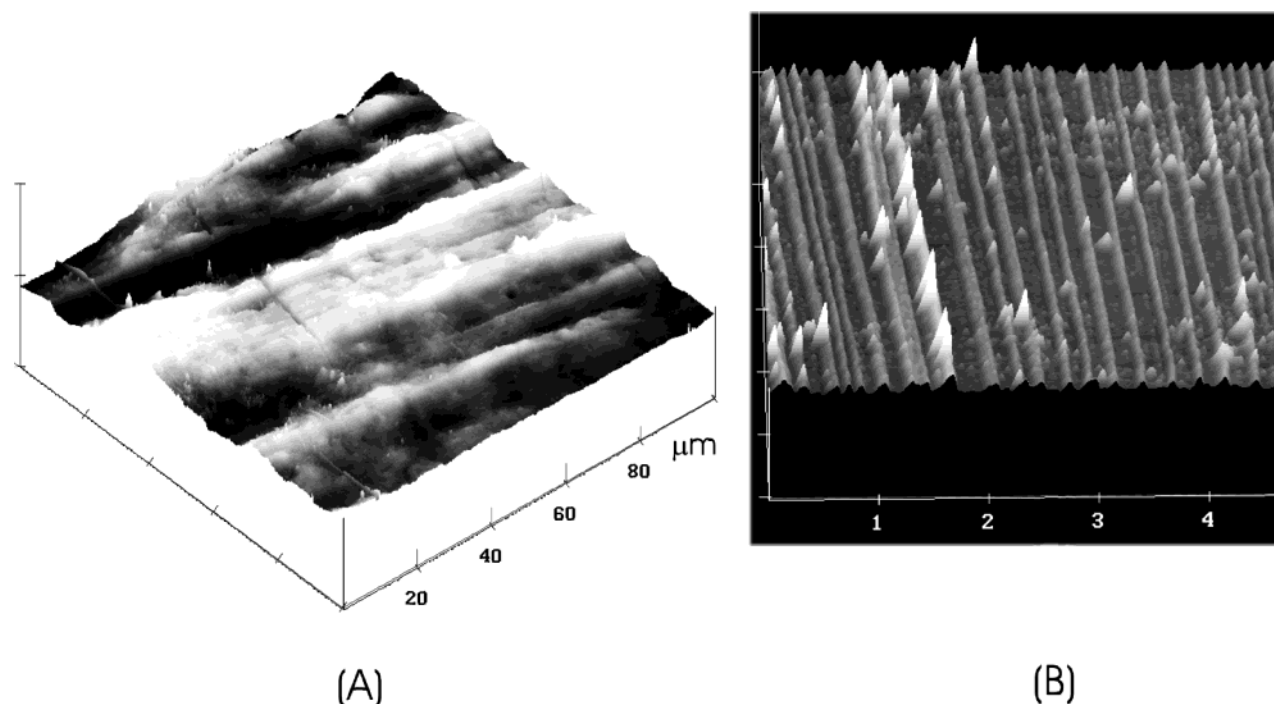
## Results and Discussion

Figure 2 shows the surface-induced  $|\psi|$  as a function of  $[C_6]$ . The orientation of the optical axis is almost parallel (with a

\* Corresponding author. E-mail: afigueiredo@if.usp.br.

<sup>†</sup> Universidade de São Paulo.

<sup>‡</sup> Politecnico di Torino and Istituto Nazionale di Fisica della Materia.



**Figure 1.** Scanning electron micrograph (SEM) of the (A) Be plate and (B) Teflon-deposited layer.

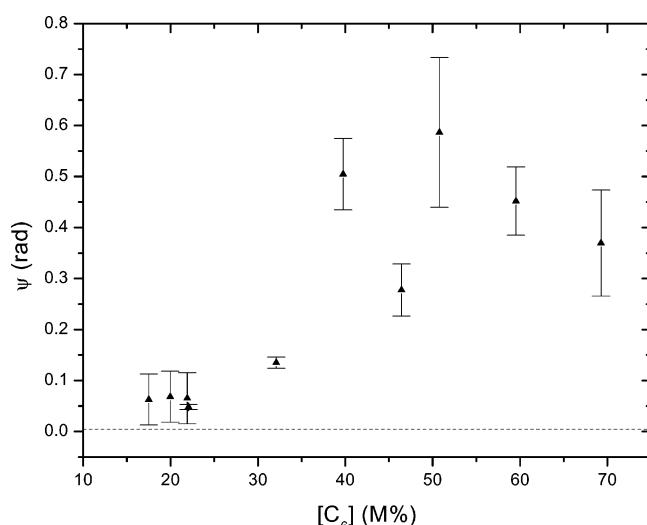


**Figure 2.** Surface-induced optical phase shift ( $\psi$ ) as a function of  $[C_6]$  of the sponge-phase samples.

spread of  $\sim 15^\circ$ ) to the direction of the channels present in the Teflon layer. The order of magnitude of  $|\psi|$  ranges over an order of magnitude from 0.05 to 0.5 rad and presents a tendency to increase as  $[C_6]$  increases.

Representative samples of the sponge phase were investigated under grazing X-ray scattering. Figure 3 shows the typical grazing diffracted intensity as a function of the modulus of the scattering vector  $q$  ( $= (2 \sin \theta)/\lambda$ , where  $2\theta$  is the scattering angle) of one of these samples. The diffraction patterns show features completely different from those obtained from the bulk of the  $L_3$  phase: several Bragg peaks are present, indicating a crystalline-like structure in the interfacial layer. The diffraction peaks are indexed to a tetragonal lattice (parameters  $a$  and  $c$ ). The ratio  $c/a$  increases (almost linearly) as  $[C_6]$  increases, from about 1 to 3 (Figure 4). Figure 5 shows the correlation distance ( $D$ ) as a function of  $[C_6]$ , obtained from the width at half-height of the grazing scattering diffraction peaks. This parameter gives an evaluation of the thickness of the surface-induced anisotropic

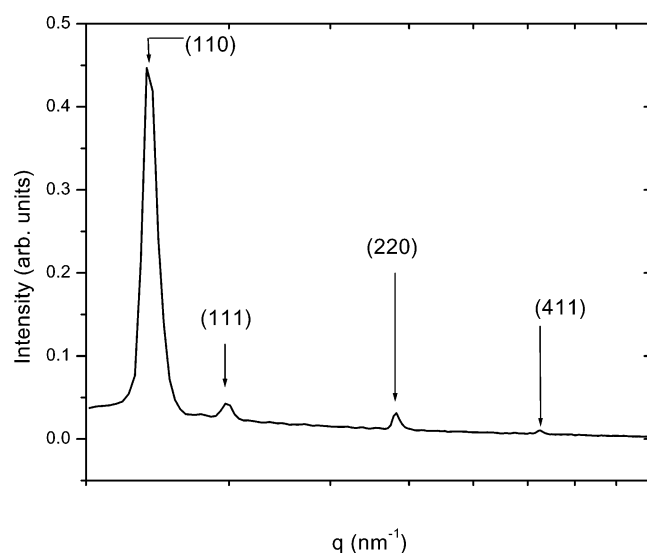


**Figure 3.** Typical grazing diffracted intensity of a sponge phase as a function of the modulus of the scattering vector  $q = \{2 \sin(\theta)\}/\lambda$ , where  $2\theta$  is the scattering angle. The numbers ( $h, k, l$ ) represent the Miller indices associated with the peaks in the indexation procedure.

layer over the Be plate. Over the entire  $[C_6]$  concentration range investigated,  $D \approx 15 \text{ nm} \approx 3a$ . At  $[C_6] \lesssim 30$ , where the viscosity of the sample is  $\nu \approx 200 \text{ cP}$ ,<sup>10</sup> the tetragonal structure induced by the surface field is almost cubic, with  $c/a \gtrsim 1$ . At  $[C_6] \gtrsim 60$ , the sample is much less viscous,  $\nu \approx 20 \text{ cP}$  and  $c/a \approx 3$ .

By comparing these lattice parameters ( $a \approx 5 \text{ nm}$  and  $5 \lesssim c \lesssim 13 \text{ nm}$ ) with the values of  $d$  and  $\delta$  of the  $L_3$  phase in the bulk, we see that the induced structure at the interface is not simply a deformation of the “melted cubic” structure present in the bulk but a deep topological metamorphosis of the structure. A possible candidate to be responsible for this phenomenon could be the selective adsorption of the different compounds of the mixture by the surface. This mechanism, which has already been proposed in the case of wetting-induced anisotropic structures in magnetic colloids,<sup>11</sup> could generate a concentration

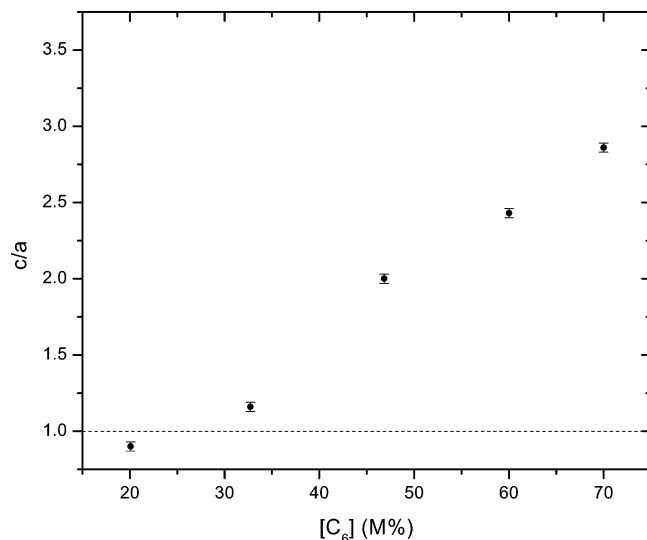


**Figure 4.**  $c/a$  as a function of  $[C_6]$ , where  $c$  and  $a$  are the lattice parameters of the tetragonal structure induced by the wetting of the Be plate by the sponge phase.

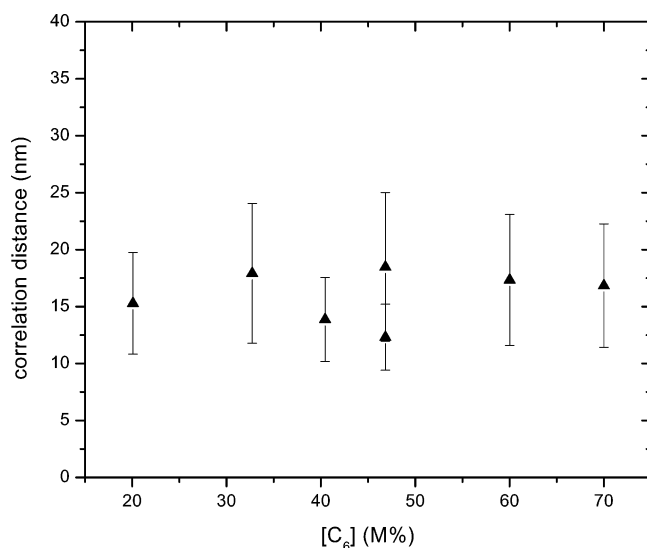


**Figure 5.** Correlation distance as a function of  $[C_6]$ , obtained from the width at half-height of the grazing scattering diffraction peaks.

gradient of compounds from the surface to the bulk, inducing the tetragonal structure observed. This aspect will be discussed in more detail in the next section.

**Phenomenological Adsorption Model. General Features.** In this section, we will show that the observed surface-induced birefringence can be interpreted as a mechanical deformation induced on the surface electric field due to selective ion adsorption.

Let us assume that the sponge phase has, locally, a melted cubic structure. In an actual bicontinuous lyotropic cubic phase (Q) structure,<sup>12,13</sup> there is a lattice that can be identified. In a first-order approximation, we superimpose over the corresponding bicontinuous sponge structure a regular cubic array of lattice points in an isotropic liquid. These lattice points should be pictured as the loci (vertexes) where the solvent channels meet each other almost perpendicularly, as in the case of the cubic lyotropic phases. The difference between the Q- and the L<sub>3</sub>-phase structures, at this point, is the lack of long-range ordering in the sponge phase. In the bulk, in the absence of distorting fields, the medium behaves optically isotropically. Close to a substrate, a surface field can break the bulk isotropy and induce

a surface phase that is optically anisotropic. If the surface field has a component just along the geometrical normal to the surface, then this direction will be a symmetry axis of the structure. However, if the surface field also has a component parallel to the substrate, then optical birefringence can be observed even under normal incidence conditions for the light (linearly polarized) beam.

The physical origin of this surface field should be connected with the selective ion adsorption of the substrate in contact with the sample. The component of the electric field parallel to the surface is due to a modulation of the physical properties of the substrate due to the presence of surface grooves, as shown by the SEM pictures (Figure 1). This modulation is responsible for a nonhomogeneous adsorption giving rise to a tilted electric field, whose spatial periodicity is on the order of magnitude of that of the surface topology. The effect of this electric field is to modify the unit cell of the (almost) cubic phase. The deformation minimizes the free energy of the system and has two contributions: (i) one connected with the surface interaction with the isotropic liquid around the lattice points of the sponge structure and (ii) another one with the electric polarization induced by the surface electric field. As will be shown in the following discussion, the shape of equilibrium of the “deformed lattice” is tetragonal, with one of the symmetry axes parallel to the surface field.

#### Main Characteristics of the Surface Field of Ionic Origin.

Let us consider a liquid (for example, a lyotropic liquid crystal) with ions dissolved on it, limited by a flat surface. These ions can be due to the presence of impurities or to the ionization of the molecules present in the liquid (e.g., ionic heads of lyotropic molecules). The adsorption energy of a charge  $Q$  by the substrate is given by the interaction of the ion with its image in the substrate. It can be written as<sup>14</sup>

$$\epsilon_{\text{ads}} = \frac{Q^2}{8\pi R} \frac{1}{\epsilon(\epsilon + \epsilon_s)} \quad (1)$$

where  $\epsilon$  is the dielectric constant of the liquid crystal,  $\epsilon_s$  is the dielectric constant of the substrate, and  $R$  is the geometrical dimension of the ion. Usually the positive and negative ions have different geometrical dimensions. Consequently there is a selective adsorption of ions of a given electric charge sign. This selective adsorption is responsible for an electric field localized close to the limiting surface over a few Debye screening lengths.<sup>15</sup>

The SEM pictures show that the substrates considered in our experimental investigation, shown in Figure 1, present a periodic structure. In this case, the adsorption is not homogeneous on the surface, and the electric field is expected to be tilted with respect to the direction perpendicular to the substrate surface.

The electric potential ( $\phi$ ) in the liquid containing ions, according to the Poisson–Boltzmann model, is given by

$$\frac{\partial^2 \phi}{\partial x^2} + \frac{\partial^2 \phi}{\partial z^2} = \frac{1}{\lambda^2} \phi \quad (2)$$

where  $x$  and  $z$  are the coordinates in the surface and perpendicular to it, respectively, and  $\lambda$  is the Debye screening length. Equation 2 holds if  $\phi < k_B T / Q \approx 25$  mV, where  $k_B$  and  $T$  are the Boltzmann constant and the temperature, respectively.

We assume that the surface charge density of adsorbed ions is given by

$$\sigma(x) = \sigma_m + \sigma_0 \cos(kx) \quad (3)$$

where  $\sigma_m$  is the average value of the surface adsorbed charge, which depends on the adsorption energy. The remaining term takes into account the modulation of the adsorbed charge connected with the geometrical surface structure, whose macroscopic wavelength is  $\Lambda$ .  $k = 2\pi/\Lambda$  is the wave vector of the surface structure, directed along the  $x$  axis. In this framework, the electric potential is

$$\phi(x, z) = \phi_m \exp(-z/\lambda) + \phi_0 \cos(qx) \exp(-z/l) \quad (4)$$

where the constants  $\phi_m$  and  $\phi_0$  have to be determined in terms of  $\sigma_m$  and  $\sigma_0$  and

$$l = \frac{\lambda}{\sqrt{1 + (k\lambda)^2}} \quad (5)$$

We note that if  $\Lambda \gg \lambda$  then one has  $l \approx \lambda$ . Because in our case  $\lambda$  is in the range of nanometers, whereas  $\Lambda$  is in the range of 0.2–10  $\mu\text{m}$ , it follows that  $l \approx \lambda$  for the two substrates (Be and Teflon) experimentally investigated.

Using the boundary condition  $\mathbf{E} \cdot \mathbf{z} = \sigma/\epsilon$  at  $z = 0$ , we obtain  $\phi_m = \sigma_m \lambda / \epsilon$  and  $\phi_0 = \sigma_0 l / \epsilon$ . From this analysis, it follows that the  $x$  component of the electric field due to the adsorption phenomenon exists only if there is a modulation of the adsorbed charge. In the opposite case (without this surface modulation), the electric field is parallel to the unit vector  $\mathbf{z}$  (perpendicular to the substrate). The average value of  $E^2 = E_x^2 + E_z^2$  over  $\Lambda$  along the  $x$  axis is then

$$\langle E^2 \rangle = \frac{1}{\Lambda} \int_0^\Lambda E^2 dx$$

$$\langle E^2 \rangle = \left( \frac{\sigma_m}{\epsilon} \right)^2 \exp(-2z/\lambda) + \frac{1 + (kl)^2 (\sigma_0)^2}{2} \exp(-2z/l) \quad (6)$$

We note that the electric field is localized close to the limiting surface over a surface layer whose thickness is on the order of  $l \approx \lambda$ .

**Surface-Field Mechanical Deformation.** We can now evaluate the mechanical deformation induced by the surface field on the (melted) cubic structure. Let us consider an isotropic object of volume  $V$  and mass density  $\rho$  in a liquid. The surface tension between the object and the liquid is  $\gamma$ . The free energy ( $F$ ) of this object presents a bulk and a surface term<sup>14</sup>

$$F = \int_V f dv + \int_S \gamma ds \quad (7)$$

where  $f$  is the bulk energy density of the object of volume  $V$  and surface  $S$ . In the absence of an external constraint, the shape of the object is obtained by minimizing  $F$ , taking into account that its total mass  $M$  is fixed. In the following discussion, we will assume that the medium forming this object is an incompressible liquid. In this framework, the bulk contribution to  $F$  reduces to a constant. Consequently, in the absence of external constraints, the actual shape of the body is the one having the smallest surface. As is well known, in this case the shape of the object is spherical with a radius of  $R = (3M/4\pi\rho)^{1/3}$ . Let us assume now that the object is subjected to an electric field that in the absence of the object is  $\mathbf{E} = E\mathbf{u}_E$ , where  $\mathbf{u}_E$  is a unit vector parallel to the local electric field. The field polarizes the object and deforms it. The deformed object has ellipsoidal symmetry, with one of the principal axes parallel to  $\mathbf{u}_E$ . Let us indicate by  $a$ ,  $b$ , and  $c$  the semiaxes of the ellipsoidal object.

Because there is cylindrical symmetry around  $\mathbf{u}_E$ , two semiaxes are identical. We use a Cartesian reference frame having the  $\xi$  axis parallel to  $\mathbf{u}_E$ . In this case,  $a = b$ , and we assume also that  $c > a$ .

The electric contribution to the total free energy is

$$F_E = -\frac{1}{2} \mathcal{P} \mathbf{E} = -\frac{1}{2} \mathcal{P} E \quad (8)$$

because the total dipole moment  $\mathcal{P}$  of the object is parallel to the field  $\mathbf{E}$ . We note that the actual electric field distribution in the presence of the object is different from the one in the absence of it,  $\mathbf{E}$ . However, the electrostatic energy of the ellipsoidal object can be expressed in terms of  $\mathbf{E}$  only, as discussed in ref 14. The total free energy of the object in the presence of the external field is then

$$F = \int_V f dv + \gamma S - \frac{1}{2} \mathcal{P} E \quad (9)$$

The actual shape of the object is the one minimizing  $F$  given by eq 9, which satisfies the condition that  $M = \text{constant}$ . Because the medium forming the object is supposed to be incompressible, the first contribution to  $F$  given by eq 9 is a constant, and the minimum of  $F$  coincides with the minimum of

$$F_S = \gamma S - \frac{1}{2} \mathcal{P} E \quad (10)$$

For an object of ellipsoidal shape with  $c > a = b$ , the surface is given by  $S = 2\pi a[a + (c/e) \arctan(c/e)]$ , where  $e = \sqrt{1 - (a/c)^2}$  is its eccentricity. Because the object is assumed to be made of an incompressible liquid, its volume ( $V_0 = (4/3)\pi R^3$ ) in the absence of the electric field coincides with the one in the presence of the field ( $V = (4/3)\pi c a^2$ ). Consequently,  $c = R^3/a^2$ , and  $e = e(a, R)$ .

The dipole moment induced by the external field on the ellipsoidal object is<sup>14</sup>

$$\mathcal{P} = \epsilon_0 \frac{q_e - 1}{1 + (q_e - 1)n} V E \quad (11)$$

$q_e = \epsilon/\epsilon_e$ , and

$$n = \frac{1 - e^2}{2e^3} \left\{ \log\left(\frac{1 - e}{1 + e}\right) - 2e \right\} \quad (12)$$

is the depolarization factor. Instead of considering the free energy  $F_S$  given by eq 10, it is more convenient to analyze the nondimensional quantity

$$\mathcal{F}_S = \frac{F_S}{\gamma S_0} = \frac{S}{S_0} - \frac{1}{2} \epsilon_0 \frac{q_e - 1}{1 + (q_e - 1)n} \frac{V}{\gamma S_0} E^2 \quad (13)$$

where  $S_0 = 4\pi R^2$  is the surface of the object in the absence of the external electric field. Because  $V/S_0 = R/3$ , the electrical contribution to  $\mathcal{F}_S$  is

$$\frac{1}{6\gamma} \epsilon_0 \frac{q_e - 1}{1 + (q_e - 1)n} E^2 R \quad (14)$$

It follows that the quantity

$$R_c = 6 \frac{\gamma}{\epsilon_0} \frac{1 + (q_e - 1)n}{q_e - 1} \frac{1}{E^2} \quad (15)$$



has the dimension of length and can be called the electric capillary length.<sup>14</sup>

To analyze the shape of the object in the presence of the external electric field, we use  $a = R(1 - \eta)$  and analyze the dependence of  $\mathcal{F}_S = \mathcal{F}_S(\eta)$  with respect to  $\eta$ . Because in the electrical contribution to  $\mathcal{F}_S$  the shape of the body is present only in the depolarization factor  $n$ , we write eq 13 in the form

$$\mathcal{F}_S = \frac{S}{S_0} - \beta \frac{q_e - 1}{1 + (q_e - 1)n} \quad (16)$$

where

$$\beta = \frac{1}{6\gamma} \epsilon_0 R E^2 \quad (17)$$

We identify the external electric field with the one due to selective ion adsorption, evaluated at the surface  $E = \sigma/\epsilon$ . Let us assume that  $\sigma \approx 10^{-2}$  C/m<sup>2</sup>,<sup>15</sup>  $\epsilon \approx 10\epsilon_0$ ,<sup>18</sup>  $R \approx 6 \times 10^{-9}$  m, and  $\gamma \approx 2 \times 10^{-5}$  J/m<sup>2</sup>, on the order of the surface tension of the nematic phase of the MBBA in contact with its isotropic phase.<sup>17</sup> With these values, the function  $\mathcal{F}_S = \mathcal{F}_S(\eta)$ , for  $q_e \approx 3$ , has a minimum for  $\eta \approx 0.25$ , corresponding to  $c/a \approx 3$ , in agreement with our experimental X-ray data.

**Evaluation of the Induced Optical Phase Shift.** Let us evaluate now if this anisotropy observed in the tetragonal structure accounts for the optical phase shift measured. Assuming a dielectric prolate ellipsoid of semiaxes  $a$  and  $c$  in the presence of an optical field, the anisotropy of electric permittivity can be written as<sup>19</sup>

$$|\sqrt{\epsilon_{\parallel}} - \sqrt{\epsilon_{\perp}}| = \left| \frac{\sqrt{\epsilon_0 e^2}}{4} \frac{a^3 - c^3}{ca^2} \right| \quad (18)$$

where  $\parallel$  and  $\perp$  represent parallel and perpendicular to the long axis of the ellipsoid, respectively;  $\epsilon_0$  is the permittivity of free space, and  $e^2 = 1 - (a/c)^2$ . The optical phase shift can be calculated from the anisotropy of electric permittivity as

$$|\psi| = \frac{2\pi}{\lambda_1 \sqrt{\epsilon_0}} \int |\sqrt{\epsilon_{\parallel}} - \sqrt{\epsilon_{\perp}}| dz \approx \frac{\pi e^2 L (c^3 - a^3)}{2ca^2 \lambda_1} \quad (19)$$

where  $\lambda_1$  and  $L$  are the light wavelength and the optical path width, respectively. Substituting numbers into eq 19 ( $a = 4.3$  nm,  $c = 12.1$  nm,  $\lambda_1 = 632.8$  nm, and  $L \approx D = 10$  nm), we find  $|\psi| \approx 10^{-1}$  rad, which agrees, in the order of magnitude, with the values of  $|\psi|$  measured in the optical experiment with the Teflon-deposited film. This result seems to indicate that despite the fact of different substrates (Teflon and Be) with channels of different length scales the wetting of these substrates with a sponge phase induces the same type of structure in a layer at the interface. In this sense, the wetting property of the

sponge phase could be considered to be an intrinsic characteristics of the  $L_3$  phase. Our results differ from those observed in the wetting of solid substrates with thermotropics,<sup>6-8</sup> where quasi-1D, 2D, and even 3D structures were identified.

## Conclusions

In summary, we show that the wetting of a substrate with the sponge phase promotes the formation of an anisotropic layer with tetragonal symmetry on a length scale of  $\sim 10$  nm on the substrate. The topology of the substrate defines the orientation of the symmetry axis of this induced surface layer. The shape anisotropy characteristics of the tetragonal lattice experimentally obtained account for the optical phase shift measured.

In our discussion, we identify the surface field with the one due to the selective ionic adsorption as the candidate responsible for the observed change of structure from melted cubic to tetragonal.

**Acknowledgment.** Fundação de Amparo à Pesquisa do Estado de São Paulo supported this work. We thank Dra. M. C. Salvadori for the SEM pictures.

## References and Notes

- (1) Porte, G.; Marignan, J.; Bassereau, P.; May, R. *J. Phys. (France)* **1988**, *49*, 511.
- (2) Roux, D.; Cates, M. E.; Olsson, U.; Ball, R. C.; Nallet, F.; Bellocq, A. M. *Europhys. Lett.* **1990**, *11*, 229.
- (3) Balinov, B.; Olsson, U.; Söderman, O. *J. Phys. Chem.* **1991**, *95*, 5931.
- (4) Magalhães, M.; Pusiol, D.; Ramia, M. E.; Figueiredo Neto, A. M. *J. Chem. Phys.* **1998**, *108*, 3835.
- (5) Magalhães, M.; Figueiredo Neto, A. M.; Tolédano, P. *Phys. Rev. E* **2000**, *62*, 5847.
- (6) Dai, P.; Wang, S. K.; Taub, H.; Buckley, J. E.; Ehrlich, S. N.; Larese, J. Z.; Binning, G.; Smith, D. P. E. *Phys. Rev. B* **1993**, *47*, 7401.
- (7) Lacaze, E.; Alba, M.; Barré, J.; Braslau, A.; Goldmann, M.; Serreau, J. *Physica B* **1998**, *248*, 246.
- (8) Michel, J. P.; Lacaze, E.; Alba, M.; Goldmann, M.; Rieutord, F. *Surf. Sci.* **2002**, *507-510*, 374.
- (9) Fabre, P.; Casagrande, C.; Veyssie, M. *Phys. Rev. Lett.* **1990**, *64*, 539.
- (10) Magalhães, M.; Figueiredo Neto, A. M.; Tromba, A. C. Submitted for publication.
- (11) Magalhães, M.; Figueiredo Neo, A. M.; Bee, A.; Bourdon, A. *J. Chem. Phys.* **2000**, *113*, 10246.
- (12) Luzzati, V.; Spegt, P. A. *Nature* **1967**, *215*, 701.
- (13) Mariani, P.; Luzzati, V.; Delacroix, H. *J. Mol. Biol.* **1988**, *204*, 165.
- (14) Landau, L.; Lifchitz, E. *Electrodynamique des Milieux Continus*; MIR: Moscow, 1969.
- (15) Israelachvili, J. *Intermolecular and Surface Forces*; Academic Press: San Diego, CA, 1992.
- (16) Landau, L. D.; Lifchitz, E. I. *Fluids Mechanics*; MIR: Moscow, 1968.
- (17) Sheng, P. In *Introduction to Liquid Crystals*; Priestly, E. B., Wojtowicz, P. J., Sheng, P., Eds.; Plenum Press: New York, 1975.
- (18) Tsykalo, A. L. *Thermophysical Properties of Liquid Crystals*; Gordon & Breach, New York, 1991.
- (19) Stratton, J. A. *Electromagnetic Theory*; McGraw-Hill: New York, 1941.